INFECTION AND IMMUNITY, Aug. 1987, p. 1784–1791
0019-9567/87/081784-08$02.00/0

Vol. 55, No. 8

Influence of Type and Opsonization of Ingested Particle on Intracellular Free Calcium Distribution and Superoxide Production by Human Neutrophils

TEIZO MURATA, JAMES A. SULLIVAN, DANIEL W. SAWYER, AND GERALD L. MANDELL*

Division of Infectious Diseases, Department of Medicine, University of Virginia School of Medicine, Charlottesville, Virginia 22908

Received 13 February 1987/Accepted 2 April 1987

Intracellular free calcium concentration ($[Ca^{2+}]_i$) was measured with the fluorescent Ca^{2+} indicator Fura 2 within individual human neutrophils during the phagocytosis of several types of particles, including serum-treated zymosan (STZ), immunoglobulin G (IgG)-coated zymosan (IGZ), C3b-coated zymosan (C3Z), nontreated zymosan (Z), and serum-treated similarly sized latex particles (STL). STZ was coated with both IgG and C3b. IGZ was coated with only IgG, and C3Z was coated with only C3b. STL was coated with only C3b but to a lesser extent than C3Z. The ingestion of particles was greatest for STZ and somewhat lower for C3Z. Ingestion of IGZ and STL was much less than ingestion of C3Z. The relative efficiencies of the particles for inducing superoxide production were as follows: STZ > IGZ = C3Z > Z = STL. $[Ca^{2+}]_i$ significantly increased from the resting level of ~70 to >240 nM ($P < 0.01$) during phagocytosis of the particles. The increment in $[Ca^{2+}]_i$ was greater in the paraphagosomal region than in the cell body after the ingestion of STZ or IGZ. The mean peak $[Ca^{2+}]_i$ values in the paraphagosomal cytoplasm of neutrophils ingesting one particle of STZ, IGZ, C3Z, Z, and STL were 536.1 ± 57.6, 424.7 ± 55.8, 373.8 ± 62.7, 272.3 ± 31.5, and 270.8 ± 38.0 nM, respectively, which showed good correlation ($r = 0.97$) with the efficiency of the particles for inducing superoxide production. Depletion of extracellular Ca^{2+} by EGTA [ethylene glycol-bis(β-aminoethyl ether)-*N*,*N*,*N*′,*N*′-tetraacetic acid] attenuated both $[Ca^{2+}]_i$ increase and superoxide production induced by particles. Thus $[Ca^{2+}]_i$ increased after ingestion of several types of particles, and the subcellular pattern of $[Ca^{2+}]_i$ was different depending on the type of particle ingested. Greater increases in paraphagosomal $[Ca^{2+}]_i$ were closely associated with greater increases in superoxide production by neutrophils.

Intracellular free calcium ($[Ca^{2+}]_i$) is thought to be an important second messenger for many neutrophil functions, including phagocytosis (28), respiratory burst (22), and degranulation (27). To elucidate the effect of intracellular free calcium on neutrophil function, several studies have been performed with the soluble stimuli, *N*-formyl-methionyl-leucyl-phenylalanine (21), C5a (6), or concanavalin A (12). However, few data are available for particulate stimuli and the effect of ingestion of these particles on intracellular $[Ca^{2+}]_i$ patterns. To better understand the role of Ca^{2+} in neutrophil activation, we measured and visualized $[Ca^{2+}]_i$ after ingestion of particles and correlated these $[Ca^{2+}]_i$ patterns with neutrophil oxidative activity.

Ingestion of latex particles by neutrophils causes a weak oxidative response compared with ingestion of particles of similar size, such as *Staphylococcus aureus*, when the same number of particles is ingested per neutrophil (16). Roos et al. (23) observed that ingestion of zymosan particles coated with immunoglobulin G (IgG), C3, or both enhanced the oxidative metabolism of neutrophils but that ingestion of unopsonized zymosan particles did not.

We recently reported measuring and visualizing $[Ca^{2+}]_i$ within single living cells using Quin 2 as a fluorescent Ca^{2+} indicator (26). Fura 2, more recently developed by Grynkiewicz and co-workers (9), is superior to Quin 2 as a Ca^{2+} indicator because it binds to Ca^{2+} more specifically and possesses ~30 times stronger fluorescence intensity than Quin 2, allowing more precise measurement of $[Ca^{2+}]_i$ without interfering with phagocyte functions. In the present study, we examined $[Ca^{2+}]_i$ distribution using Fura 2 during the phagocytosis of several types of particles and related this to superoxide production by human neutrophils.

MATERIALS AND METHODS

Reagents. Ficoll-Histopaque 1077, superoxide dismutase, cytochrome *c* (type IV), EGTA [ethylene glycol-bis(β-aminoethyl ether)-*N*,*N*,*N*′,*N*′-tetraacetic acid], and human serum albumin were purchased from Sigma Chemical Co., St. Louis, Mo. Hanks balanced salt solution (HBSS) was from M. A. Bioproducts, Walkersville, Md. Zymosan particles were from Schwartz Mann, Spring Valley, N.Y. Latex particles were from Polyscience, Inc., Warrington, Pa. Fura 2 acetoxymethyl ether, ionomycin, human IgG, and fluorescein-conjugated anti-human IgG were obtained from Calbiochem-Behring, La Jolla, Calif. Fluorescein-conjugated anti-human C3c was from Behring Diagnostics, La Jolla, Calif.

Isolation of human neutrophils. Neutrophils (95% pure) were isolated from heparinized (10 U/ml) venous blood of normal volunteers by Ficoll-Hypaque separation (3), followed by dextran sedimentation and hypotonic lysis of erythrocytes (5).

Opsonization of particles. Serum-treated zymosan (STZ; 4- to 7-μm diameter) and serum-treated latex (STL; 4.1-μm diameter) were prepared by incubating zymosan or latex particles with 50% fresh autologous serum in HBSS at 37°C

* Corresponding author.

for 30 min at a concentration of 1×10^8 to 4×10^8 particles per ml. IgG-coated zymosan (IGZ) was prepared by incubating zymosan with human IgG (5 mg/ml) in HBSS at 37°C for 30 min at a concentration of 10^9 particles per ml.

C3b-coated zymosan (C3Z) was prepared by the method of Roos et al. (23). After the addition of disodium EDTA (pH 7.4) at a final concentration of 10 mM to fresh autologous serum, zymosan-specific immunoglobulins were removed by incubating the serum with zymosan (30 mg/ml) twice at room temperature for 30 min; the serum was then recalcified with 0.1 ml of 100 mM $CaCl_2$ per ml of serum. Then zymosan was incubated with absorbed serum at 37°C for 30 min at a concentration of 1×10^8 to 4×10^8 particles per ml.

Unopsonized zymosan (Z) and unopsonized latex (L) were prepared by incubating zymosan or latex with HBSS at 37°C for 30 min. All particle types were washed with HBSS after opsonization and kept on ice until use. Particles were counted with a hemacytometer and diluted to an appropriate concentration with HBSS.

Measurement of IgG and C3b on particles. The amount of IgG and C3b on zymosan or latex particles was measured with fluorescein-conjugated anti-human IgG or anti-human C3c. The C3c fragment of C3b is an important fragment for the opsonization of particles, and anti-C3c has been used to quantitate C3b (29). Each type of particle was incubated with fluorescein-conjugated anti-IgG or anti-C3c at a particle concentration of 10^6/ml at 37°C for 30 min. The particles were washed two times with HBSS and observed with a Leitz Orthoplan microscope equipped with a 100-W mercury vapor epi-illuminator, glycerine immersion objective (Nikon 100× UV-CF), silicon-intensified target camera (DAGE series 65; PAGE-MTI, Inc., Michigan City, Ind.), and optical cube (Leitz H2 cube; excitation, 390 to 490 nm; emission, >515 nm). The fluorescence images of each type of particle were stored on video tape, and the fluorescence intensity of each particle was quantitated by digital image analysis (Quantex 9210). The relative amounts of IgG and C3b fixed on particles were calculated by dividing the digitized fluorescence intensity of each particle by the molar fluorescence/protein ratio (F/P ratio) of fluorescein-conjugated anti-IgG (F/P = 3.5) or anti-C3c (F/P = 2.5). The molar amount of IgG fixed on STZ was 30% of that of C3b.

Measurement of superoxide production. Superoxide production was measured by determining the superoxide dismutase-inhibitable reduction of cytochrome *c* at 550 nm (2). Neutrophils (2×10^6 to 4×10^6 cells per ml) were suspended with HBSS containing cytochrome *c* and then incubated with particles at various particle/cell ratios in a shaking water bath at 37°C for 10 min. Superoxide dismutase was added to each control mixture, which had been prepared in a manner identical to that for the reaction mixtures. After centrifugation of both control and reaction mixtures at 1,500 × *g* for 15 min at 4°C, cytochrome *c* reduction was determined by measuring the A_{550} of each supernatant. At the end of the incubation, 50-μl portions of the reaction mixture were removed for phagocytosis assay.

Phagocytosis assay. At the end of the incubation of superoxide production, 50-μl portions of the reaction mixture were removed from each tube and mixed with 2 ml of ice-cold HBSS. The cells with the ingested particles were washed two times with ice-cold HBSS with a Vortex mixer. Smears were made by using a cytocentrifuge (Shandon Southern Instruments, Inc., Sewickley, Pa.). After Giemsa staining of the cells, the number of microscopically determined intracellular particles were enumerated in 50 to 100 neutrophils.

Fura 2 loading. Neutrophils (1×10^6 to 2×10^6 cells per ml) were incubated with HBSS containing Fura 2 acetoxymethyl ester at a concentration of 5 to 10 μM for 60 min at 37°C. After incubation, the cells were washed with HBSS and held at room temperature for 2 h, allowing hydrolysis of the ester to the active Ca^{2+} indicator. The free Fura 2 concentration in the loaded cells was 0.9 to 1.3 mM, assuming that the cell volume was 0.35 μl/10^6 cells (6). Superoxide production by the cells was not altered by loading with Fura 2 at this concentration (data not shown).

Fluorescence microscopy. Fluorescence microscopy was performed as previously described (26) with slight modifications. Fura 2-loaded neutrophils (10^5 cells), suspended with HBSS containing 5% human serum albumin, were allowed to attach to cover slips by incubation at 37°C for 15 to 30 min. After incubation, the cover slips were inverted on glass slides spread with 10^6 particles and the cover slip edges were secured with a 1:1 mixture of petroleum jelly and melted paraffin. For experiments without extracellular Ca^{2+}, cover slips with the attached Fura 2-loaded neutrophils were incubated in Ca^{2+}-free HBSS containing 5 mM EGTA and 0.8 mM $MgSO_4$ at 37°C for 1 min just before microscopy. Particles were also washed and suspended with Ca^{2+}-free HBSS containing 5 mM EGTA and 0.8 mM $MgSO_4$.

The cells were examined with a Leitz Orthoplan microscope equipped with a 100-W mercury epi-illuminator and glycerine immersion objective (Nikon 100× UV-CF). Neutrophils to be used for analysis were selected by bright-field microscopy. Images of single cells were collected in triplets with a silicon-intensified target camera (DAGE series 65) and stored for later processing with a Quantex 9210 image processor. The first image was a bright-field image. The second and third images were fluorescence images obtained with a long-pass barrier filter that transmits wavelengths greater than 510 nm. The cells were excited first at 340 nm (10-nm half width) and subsequently at 380 nm (10-nm half width paired with a 50% transmission neutral density filter). The two fluorescence images were separated in time by less than 0.5 s. To determine the peak $[Ca^{2+}]_i$, images of a single cell were recorded at 15- to 30-s intervals for at least 3 min during and after phagocytosis of a particle.

Quantitation of $[Ca^{2+}]_i$. Each fluorescence image was converted to a pixel array (640 by 480 by 8 bits). The paraphagosomal region was defined as the area of the neutrophil within an approximately 3-μm periphery from the edge of the attached or ingested particle. The cell body was defined as the portion of the cell posterior to the paraphagosomal area. Three areas (ca. 1 μm^2) were chosen appropriately in both the paraphagosomal region and the cell body on the bright-field image. Density readings of these areas were taken at the corresponding pixels within both 340- and 380-nm fluorescence images. The ratio of fluorescence intensity at 340 nm to that at 380 nm was calculated. $[Ca^{2+}]_i$ within the appropriate area of the cell was calculated according to the following equation (9):

$$[Ca^{2+}]_i = K_d \times \frac{R - R_{min}}{R_{max} - R} \times \frac{I_{380} \text{ of } Ca^{2+}\text{-depleted cells}}{I_{380} \text{ of } Ca^{2+}\text{-saturated cells}}$$

where K_d is the dissociation constant of Fura 2 for Ca^{2+} (assumed to be 224 nm) (9); R is the ratio of fluorescence intensity at 340 nm to that at 380 nm; R_{min} and R_{max} are the R when probe is depleted of Ca^{2+} and saturated with Ca^{2+}, respectively; and I_{380} is the fluorescence intensity at 380 nm.

Ca^{2+}-depleted and Ca^{2+}-saturated cells were prepared as follows. Neutrophils (1×10^6 to 2×10^6 cells per ml) were

TABLE 1. Relative amounts of IgG and C3b on particles[a]

Particle	Amt (%) of:	
	IgG	C3b
STZ	100	100
IGZ	95.8 ± 15.8	3.6 ± 2.3
C3Z	0.6 ± 0.4	88.0 ± 9.3
Z	0	0
STL	0	44.8 ± 19.3
L	0	0

[a] Data are expressed as means ± SEM of six experiments with different particle preparations. The fluorescence intensity of Z or L was <3% of that of STZ. Fluorescence intensity of Z was subtracted from that of STZ, IGZ, or C3Z, and fluorescence intensity of L was subtracted from that of STL. Results are indicated as the percentage of STZ. IgG, reaction with fluorescein-conjugated anti-human IgG (STZ = 100); C3b, reaction with fluorescein conjugated anti-human C3c (STZ = 100).

incubated in Ca^{2+}-free HBSS with 1 μM ionomycin and 5 mM EGTA for 10 min at 37°C, washed two times, and suspended with Ca^{2+}-free HBSS containing 5 mM EGTA. Fura 2 was loaded like the normal cells with Ca^{2+}-free HBSS containing 5 mM EGTA as the suspending buffer throughout the experiment. The R_{min} was determined by measuring the fluorescence intensity at 340 and 380 nm in >10 cells. Ca^{2+}-depleted cells were then centrifuged and suspended in HBSS containing 10 mM $CaCl_2$. Immediately after the addition of ionomycin (final concentration, 1 μM), fluorescence intensity in >10 cells was measured and the R_{max} was determined.

Visualization of $[Ca^{2+}]_i$ localization. To visually display the local $[Ca^{2+}]_i$ within a single cell, the intensity of each pixel of the two digitized fluorescence images was converted to a logarithm and the 380-nm logarithmic image was subtracted from that at 340 nm (ratio image). The antilog of the difference represents the Ca^{2+} distribution and is independent of intracellular free Fura 2 concentration and the cell thickness.

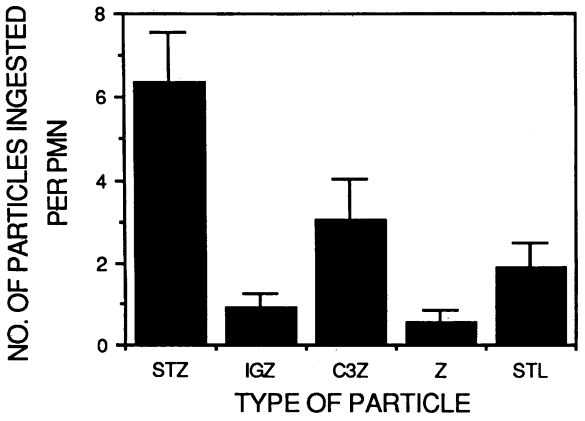

FIG. 1. Ingestion of particles by neutrophils. Neutrophils were incubated with STZ, IGZ, C3Z, Z, or STL at a particle/cell ratio of 20:1 at 37°C for 10 min. The number of microscopically determined intracellular particles was enumerated in 50 to 100 neutrophils. Data are expressed as means ± the standard error of the mean (SEM) of six experiments with different particle preparations. Significantly more STZ was ingested than the other types of particles ($P < 0.05$). The level of C3Z ingestion was significantly higher than that for IGZ, Z, or STL ($P < 0.05$).

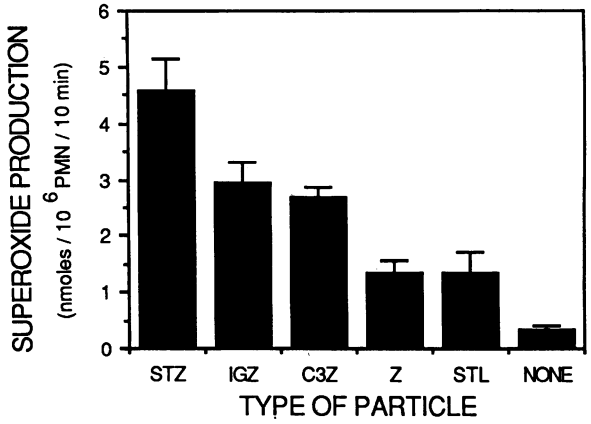

FIG. 2. Influence of particle type on superoxide production by human neutrophils. Neutrophils were incubated with STZ, IGZ, C3Z, Z, or STL at various particle/cell ratios. Superoxide production was determined by measuring the superoxide dismutase-inhibitable reduction of cytochrome *c* at 550 nm. The number of microscopically determined intracellular particles was enumerated in 50 to 100 neutrophils. Data are expressed as the amount of superoxide (mean ± SEM of five experiments) induced by five particles per cell, calculated from the regression curves of each experiment. Superoxide production of particle-ingesting cells was significantly greater than that of resting cells ($P < 0.01$). STZ, IGZ, or C3Z induced significantly more superoxide production than did Z or STL ($P < 0.01$). Furthermore, STZ induced significantly greater response than did IGZ or C3Z ($P < 0.05$).

RESULTS

Characterization of particles. As shown in Table 1, STZ was coated with both IgG and C3b. IGZ was coated with only IgG. C3Z was coated with only C3b and not with IgG. In contrast to STZ, STL was coated with only C3b. All particles in a preparation were coated homogeneously with IgG or C3b or both.

Ingestion of particles by neutrophils. The ingestion of several types of particles by neutrophils was compared at a particle/cell ratio of 20:1 (Fig. 1). Particle ingestion was greatest with STZ, followed in descending order by C3Z, STL, IGZ, and Z. This order of particle ingestion was also observed at particle/cell ratios of 10:1 or 40:1 (data not shown).

Neutrophil superoxide production induced by several types of particle. Figure 2 shows neutrophil superoxide production induced by ingesting equal numbers of several types of particles. Superoxide production was greatest for STZ, followed by IGZ, C3Z, STL, and Z.

Visualization of $[Ca^{2+}]_i$ distribution during phagocytosis of particles. $[Ca^{2+}]_i$ distribution within single cells during phagocytosis of particles was visualized as described above. Figure 3 shows bright-field images and corresponding ratio images of cells ingesting several types of particle. Photographs were taken at the time of peak paraphagosomal $[Ca^{2+}]_i$. $[Ca^{2+}]_i$ increased regionally within the area of paraphagosomal cytoplasm in neutrophils ingesting STZ or IGZ particles. In contrast, no changes in the pattern of distribution of $[Ca^{2+}]_i$ were observed within the cells ingesting C3Z, Z, or STL particles.

Quantitation of $[Ca^{2+}]_i$ during phagocytosis of particles. Peak $[Ca^{2+}]_i$ was measured in the paraphagosomal region and the cell body during phagocytosis of particles (Table 2).

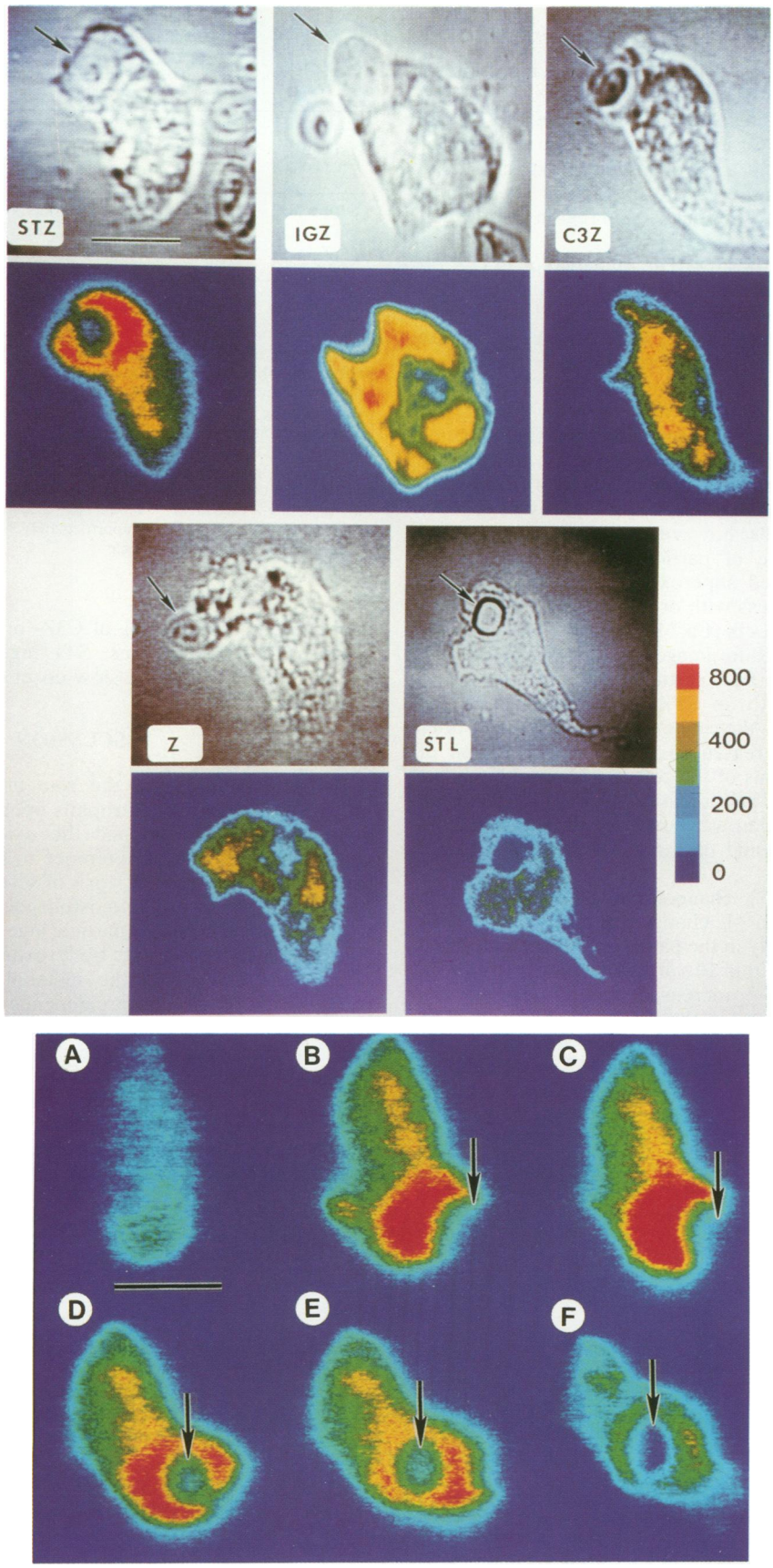

FIG. 3 and 5. 3. Visualization of $[Ca^{2+}]_i$ distribution during phagocytosis of several types of particle. Bright-field and corresponding ratio images of Fura 2-loaded neutrophils ingesting STZ, IGZ, C3Z, Z, or STL particles. The scale indicates approximate $[Ca^{2+}]_i$ in nanomoles. Arrows indicate the location of particles. Bar, 10 μm. 5. Time course of $[Ca^{2+}]_i$ distribution during phagocytosis of an STZ particle. Ratio images of a Fura 2-loaded neutrophil were taken at 15-s intervals during phagocytosis of an STZ particle. (A) Ratio image of a neutrophil migrating toward an STZ particle. Bar, 10 μm. (B to F) Ratio images of the same cell at 5 (B), 20 (C), 35 (D), 50 (E), and 65 (F) s after attachment to an STZ particle. Arrows indicate the location of the particle.

The paraphagosomal $[Ca^{2+}]_i$ levels after the ingestion of several types of particles were as follows: STZ > IGZ > C3Z > Z = STL, a finding which showed good correlation to the efficiency of the particle for inducing superoxide production. In comparison with the $[Ca^{2+}]_i$ of nonphagocytosing cells, $[Ca^{2+}]_i$ of cells ingesting any type of particle was significantly higher in both the paraphagosomal region and the cell body ($P < 0.01$).

Influence of EGTA on $[Ca^{2+}]_i$. The influence of EGTA on $[Ca^{2+}]_i$ during phagocytosis of several types of particles was examined (Table 3). The cells were suspended with Ca^{2+}-free HBSS containing 5 mM EGTA and 0.8 mM $MgSO_4$ just before the assay. This procedure did not alter the resting $[Ca^{2+}]_i$ level. In contrast, increases in $[Ca^{2+}]_i$ after the ingestion of any type of particle were markedly inhibited.

Influence of EGTA on superoxide production. The influence of EGTA on neutrophil superoxide production induced by several types of particles was examined (Fig. 4). Depletion of extracellular Ca^{2+} had no influence on superoxide production by unstimulated cells; however, superoxide production stimulated by any type of particle was decreased. The various particles induced superoxide production with the same relative effectiveness with or without EGTA.

Visualization of changes in $[Ca^{2+}]_i$ pattern during phagocytosis of STZ over time. Ratio images were taken before and after phagocytosis of an STZ particle at 15-s intervals (Fig. 5). Before attachment to an STZ particle, $[Ca^{2+}]_i$ in the polarized neutrophil was distributed evenly. Within 5 s after attachment, $[Ca^{2+}]_i$ increased markedly in the region of attachment. Other regions of the cell also showed a moderate increase in $[Ca^{2+}]_i$. The increased level of $[Ca^{2+}]_i$ within the paraphagosomal region was sustained through the completion of phagocytosis and then gradually returned to the resting level.

Quantitation of $[Ca^{2+}]_i$ changes during phagocytosis of particles over time. $[Ca^{2+}]_i$ changes during phagocytosis were measured separately in the paraphagosomal region and the cell body (Fig. 6). Within 10 s after attachment to an STZ or IGZ particle, $[Ca^{2+}]_i$ increased rapidly both in the paraphagosomal region and in the cell body and reached its peak concentration within 30 s. The elevated $[Ca^{2+}]_i$ returned gradually to the resting level by 165 s after attachment. In contrast, $[Ca^{2+}]_i$ of C3Z- or Z-ingesting cells had lower peak concentrations. STL-ingesting cells showed a low peak in $[Ca^{2+}]_i$ and a slow onset of increase in $[Ca^{2+}]_i$.

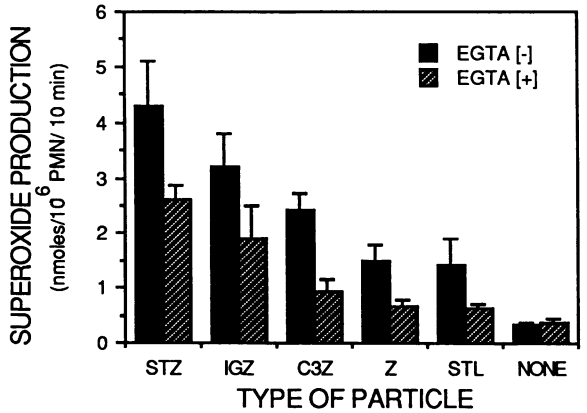

FIG. 4. Influence of EGTA on neutrophil superoxide production induced by several types of particles. Neutrophils were suspended with Ca^{2+}-free HBSS containing 5 mM EGTA and 0.8 mM $MgSO_4$ just before the assay. Data are expressed as the means ± SEM of three experiments. The same population of the cells was used for experiments with and without EGTA. EGTA significantly inhibited superoxide production induced by any type of particle ($P < 0.05$).

TABLE 2. Peak $[Ca^{2+}]_i$ during phagocytosis of several types of particle[a]

Particle	No. of cells	Intracellular free calcium (nM) in:	
		Paraphagosomal region	Cell body
None	25	69.6 ± 4.7	69.6 ± 4.7
STZ	31	536.1 ± 57.6	350.0 ± 30.2
IGZ	14	424.7 ± 55.8	358.3 ± 51.5
C3Z	12	373.8 ± 62.7	356.6 ± 57.5
Z	18	272.3 ± 31.5	282.7 ± 38.5
STL	19	270.8 ± 38.0	247.2 ± 34.0

[a] Data are expressed as the means ± SEM. Statistical analysis was performed with a paired *t* test comparing the paraphagosomal region and the cell body of the same cells or with an unpaired *t* test comparing $[Ca^{2+}]_i$ of the cells ingesting different types of particles and the resting cells. $[Ca^{2+}]_i$ increased significantly in phagocytosing cells when compared with resting cells ($P < 0.01$). With STZ or IGZ, $[Ca^{2+}]_i$ in the paraphagosomal region was significantly higher than that in the cell body ($P < 0.01$). Paraphagosomal $[Ca^{2+}]_i$ of the cells ingesting STZ or IGZ was significantly higher than that of cells ingesting Z or STL ($P < 0.01$). The paraphagosomal region was defined as the area of the cell within an approximately 3-μm periphery from the edge of the attached or ingested particle.

DISCUSSION

To better understand the role of $[Ca^{2+}]_i$ in stimulus-response coupling of neutrophils upon activation by particulate stimuli, we examined the oxidative metabolism of neutrophils with special reference to the subcellular $[Ca^{2+}]_i$ pattern during the phagocytosis of several types of particles. Mandell (16) reported that postphagocytic oxidative activity was related to the type of particle ingested. Axline and Cohn (1) obtained similar results by lysosomal enzyme release.

Our data show that the metabolic events caused by phagocytosis of particles are dependent on the nature of the particulate stimulus rather than simply membrane perturbation. Furthermore, we suggest that the difference in the magnitude of the oxidative burst is linked to the efficiency of the particle for increasing $[Ca^{2+}]_i$. In fact, the efficiency of a particle for inducing superoxide production was more closely related to the $[Ca^{2+}]_i$ increase in the paraphagosomal region ($r = 0.97$) than that in the cell body ($r = 0.81$) (Fig. 7).

TABLE 3. Influence of EGTA on peak $[Ca^{2+}]_i$ during phagocytosis of several types of particles[a]

Particle	No. of cells	Intracellular free calcium (nM) in:	
		Paraphagosomal region	Cell body
None	10	66.8 ± 11.4	66.8 ± 11.4
STZ	18	148.2 ± 17.1	119.3 ± 9.3
IGZ	10	166.2 ± 29.5	142.9 ± 24.1
C3Z	11	148.3 ± 15.6	160.8 ± 30.0
Z	9	110.0 ± 12.4	108.3 ± 10.3
STL	8	141.5 ± 16.1	117.0 ± 12.7

[a] Data are expressed as the means ± SEM. Fura 2-loaded cells were incubated in Ca^{2+}-free HBSS containing 5 mM EDTA and 0.8 mM $MgSO_4$ at 37°C for 1 min just before the assay. $[Ca^{2+}]_i$ of the cells ingesting any type of particle was significantly higher than that in the resting cells ($P < 0.05$). $[Ca^{2+}]_i$ of the paraphagosomal region of the cells ingesting STZ was significantly higher than that of the cell body ($P < 0.05$). The paraphagosomal region was defined as the area of the cell within an approximately 3-μm periphery from the edge of the attached or ingested particle.

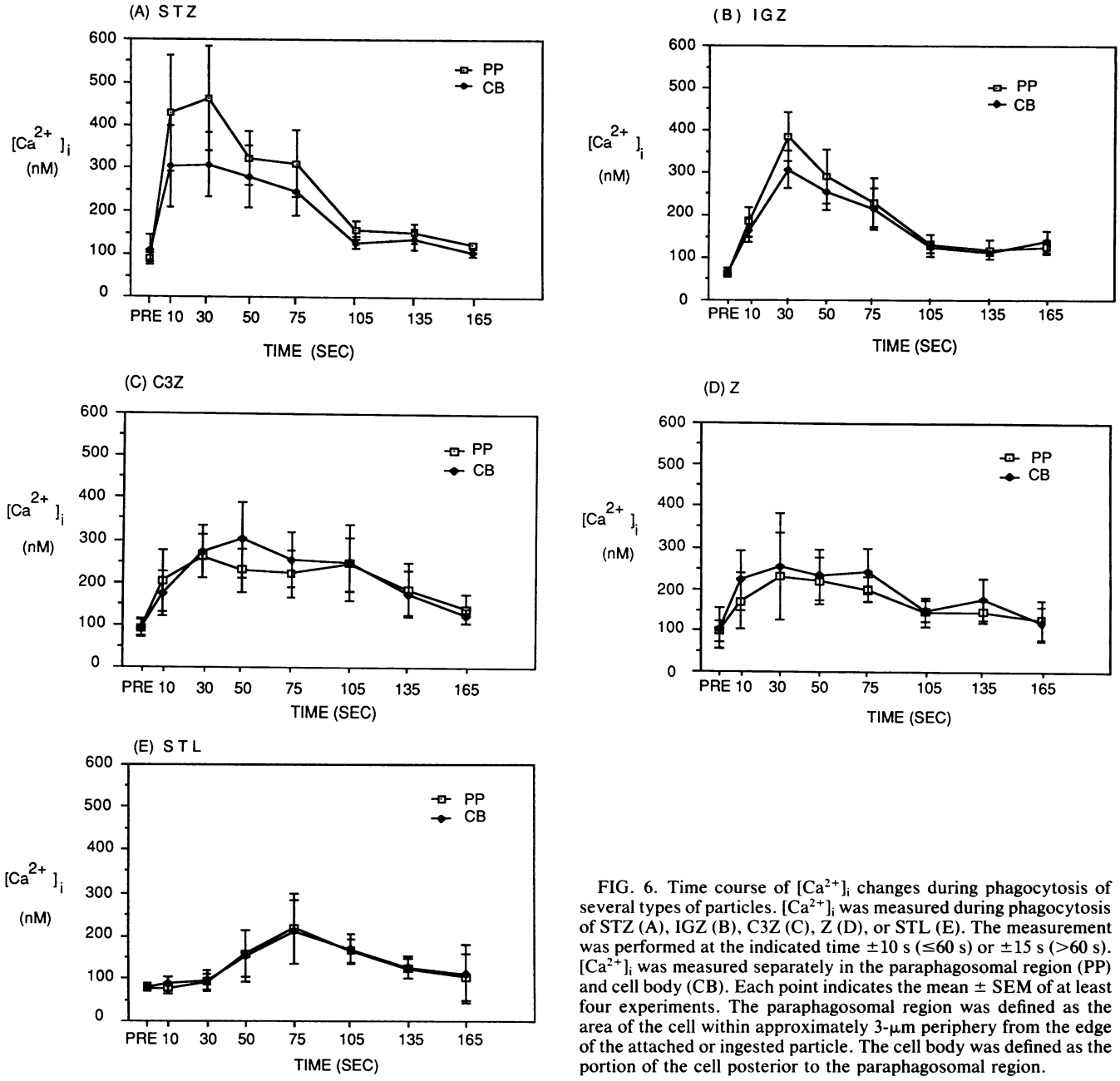

FIG. 6. Time course of [Ca^{2+}]$_i$ changes during phagocytosis of several types of particles. [Ca^{2+}]$_i$ was measured during phagocytosis of STZ (A), IGZ (B), C3Z (C), Z (D), or STL (E). The measurement was performed at the indicated time ±10 s (≤60 s) or ±15 s (>60 s). [Ca^{2+}]$_i$ was measured separately in the paraphagosomal region (PP) and cell body (CB). Each point indicates the mean ± SEM of at least four experiments. The paraphagosomal region was defined as the area of the cell within approximately 3-μm periphery from the edge of the attached or ingested particle. The cell body was defined as the portion of the cell posterior to the paraphagosomal region.

McNeil et al. (18) failed to detect an increase in [Ca^{2+}]$_i$ in macrophages with Fc-receptor-mediated phagocytosis and questioned the ability of ratio images to detect [Ca^{2+}]$_i$ changes. The present study compares Ca^{2+} patterns in which identical particles were opsonized differently. The levels of [Ca^{2+}]$_i$ observed are thus unlikely to be due to differences in cell thickness, signal/noise ratio, probe distribution, or motility.

Kruskal et al. (13) reported that [Ca^{2+}]$_i$ increased when neutrophils were spread on glass surfaces and that it returned to near resting levels within 5 min. In the present study, neutrophils were incubated to adhere to the cover slip for at least 15 min before [Ca^{2+}]$_i$ measurement. Accordingly, adhesion did not affect the measurement of resting [Ca^{2+}]$_i$. In fact, the resting [Ca^{2+}]$_i$ in the present study (69.6 nM) is almost the same as that reported by Kruskal et al. (69 nM).

The [Ca^{2+}]$_i$ values reported here, especially those for the stimulated cells, are higher than those reported in our earlier study (26) and by other investigators (6, 7, 12) but are similar to those of Lew et al. (14). We previously used Quin 2 as a fluorescent Ca^{2+} indicator and standard solutions to calibrate [Ca^{2+}]$_i$. Since Tsien et al. (31) found that increased viscosity similar to conditions of the intracellular milieu lowered the fluorescence intensity ratio of Fura 2, we used Ca^{2+}-depleted and Ca^{2+}-saturated cells to calibrate our system in the present study (see Materials and Methods).

Ca^{2+} appears to be linked to superoxide production. Ca^{2+} is reported to be necessary for the activation of protein

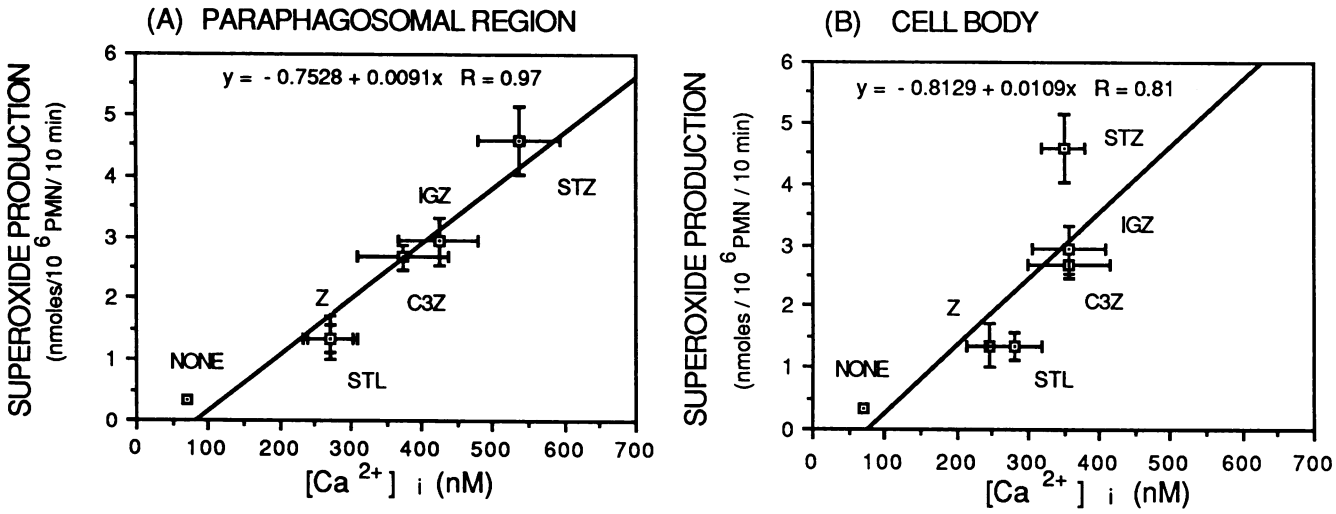

FIG. 7. Relationship between superoxide production and $[Ca^{2+}]_i$ of neutrophils ingesting several types of particles. Data are expressed as the means ± SEM. Superoxide production is plotted against paraphagosomal (A) or cell body (B) $[Ca^{2+}]_i$.

kinase C (4, 19), which leads to the activation of NADPH oxidase to induce superoxide production (4, 20). Increased $[Ca^{2+}]_i$ induces degranulation (14), which in turn promotes the translocation of cytochrome b_{254} (a putative component of the NADPH oxidase) to the phagosome membrane (10). Suzuki et al. (30) demonstrated that Ca^{2+} directly activates NADPH oxidase in membrane fractions of human neutrophils. In addition, opsonized zymosan is reported to activate the NADPH oxidase by a phospholipase A_2-mediated pathway in a Ca^{2+}-dependent manner (17). Therefore, a regional increase in $[Ca^{2+}]_i$ could result in increased oxidase activity in the paraphagosomal region. Such regional increases in paraphagosomal oxidative metabolism have been reported previously (25). The correlation demonstrated between paraphagosomal $[Ca^{2+}]_i$ and superoxide production represents an important potential mechanism for directing production of microbicidal compounds in a location optimal for destroying invading pathogens (5).

It should be noted that the opsonization of zymosan particles with both IgG and C3b greatly enhanced Ca^{2+} mobilization and superoxide production as compared with particles coated with either IgG or C3b. These data are in accord with the findings of Goldstein et al. (8), who reported that the superoxide production induced by C3-coated Sepharose beads was amplified when immunoglobulin was present on the particle surface. In addition, Roos et al. (23) observed the cooperation between C3 and IgG when fixed on the same zymosan particle in stimulating neutrophil oxygen consumption. We have shown here that IgG and C3 could interact cooperatively not only in superoxide production but also in Ca^{2+} mobilization.

In contrast to STZ, STL induced a weak Ca^{2+} mobilization and superoxide production response. This may be due to insufficient opsonization of latex particles with C3b as compared with zymosan particles (Table 1) or, more likely still, with differences between zymosan and latex. Roos et al. (23) reported that zymosan possesses specific properties for stimulating phagocytosis and lysosomal enzyme release but that latex does not. Ross et al. (24) demonstrated zymosan-specific binding sites on human neutrophils which trigger ingestion and superoxide production.

EGTA markedly inhibited $[Ca^{2+}]_i$ increase after the ingestion of particles, especially STZ, IGZ, and C3Z, indicating that the $[Ca^{2+}]_i$ increase observed was mostly from extracellular sources. In mouse macrophages, Young et al. (32) observed that the IgG Fc receptor serves as a ligand-dependent ion channel and suggested the possibility that such a channel regulates cell responses via Ca^{2+} influx. STZ and IGZ might interact with such a channel via Fc receptors to regionally increase $[Ca^{2+}]_i$.

EGTA partially decreased superoxide production induced by STZ, IGZ, or C3Z. This suggests that extracellular Ca^{2+} is not an absolute requirement for superoxide production; however, the influx of extracellular Ca^{2+} is necessary for the optimal production of superoxide induced by these types of particles. These observations are consistent with the results obtained with soluble stimuli, such as formyl-methionyl-leucyl-phenylalanine, C5a, or concanavalin A (6, 11, 12, 15, 27). In contrast to experiments performed in the presence of extracellular Ca^{2+}, the paraphagosomal $[Ca^{2+}]_i$ increase was not closely related to the superoxide induced by several types of particles in the absence of extracellular Ca^{2+} (r = 0.71; derived from the data presented in Table 3 and Fig. 4). Without extracellular Ca^{2+}, the amounts of both $[Ca^{2+}]_i$ increase and superoxide production were much smaller than those observed in the presence of extracellular Ca^{2+}. Higher levels of $[Ca^{2+}]_i$ may be necessary to enhance oxidase activity. The subcellular pattern of neutrophil $[Ca^{2+}]_i$ was different depending on the type and opsonization of the ingested particle and was directly reflected in the intensity of the oxidative burst.

ACKNOWLEDGMENT

This research was supported in part by Public Health Service grants AI09504 and T32AI07046 from the National Institutes of Health.

LITERATURE CITED

1. **Axline, S. G., and Z. A. Cohn.** 1970. In vitro induction of lysosomal enzymes by phagocytosis. J. Exp. Med. **131**:1239–1260.
2. **Babior, B. M., R. S. Kipnes, and J. T. Curnutte.** 1973. Biological defense mechanisms: the production by leukocytes of superoxide, a potential bactericidal agent. J. Clin. Invest. **52**:741–744.
3. **Boyum, A.** 1968. Isolation of mononuclear cells and granulo-

cytes from human blood: isolation of mononuclear cells by one centrifugation, and of granulocytes by combining centrifugation and sedimentation at 1 g. Scand. J. Clin. Lab. Invest. **21**(Suppl. 97):77–89.

4. **Christiansen, N. O., C. S. Larsen, and H. Juhl.** 1986. Ca^{2+} and phorbol ester activation of protein kinase C at intracellular Ca^{2+} concentrations and the effect of TMB-8. Biochim. Biophys. Acta **882**:57–62.
5. **Densen, P., and G. L. Mandell.** 1978. Gonococcal interactions with polymorphonuclear neutrophils. Importance of the phagosome for bactericidal activity. J. Clin. Invest. **62**:1161–1171.
6. **Gennaro, R., T. Pozzan, and D. Romeo.** 1984. Monitoring of cytosolic free Ca^{2+} in C5a-stimulated neutrophils: loss of receptor-modulated Ca^{2+} stores and Ca^{2+} uptake in granule-free cytoplasts. Proc. Natl. Acad. Sci. USA **81**:1416–1420.
7. **Goldman, D. W., L. A. Gifford, D. M. Olson, and E. J. Goetzl.** 1985. Transduction by leukotriene B_4 receptors of increases in cytosolic calcium in human polymorphonuclear leukocytes. J. Immunol. **135**:525–530.
8. **Goldstein, I. M., H. B. Kaplan, A. Radin, and M. Frosch.** 1976. Independent effects of IgG and complement upon human polymorphonuclear leukocyte function. J. Immunol. **117**:1282–1287.
9. **Grynkiewicz, G., M. Poenie, and R. Y. Tsien.** 1985. A new generation of Ca^{2+} indicators with greatly improved fluorescence properties. J. Biol. Chem. **260**:3440–3450.
10. **Higson, F. K., L. Durbin, N. Pavlotsky, and A. I. Tauber.** 1985. Studies of cytochrome *b*-245 translocation in the PMA stimulation of the human neutrophil NADPH-oxidase. J. Immunol. **135**: 519–524.
11. **Korchak, H. M., L. E. Rutherford, and G. Weissmann.** 1984. Stimulus response coupling in the human neutrophil. I. Kinetic analysis of changes in calcium permeability. J. Biol. Chem. **259**: 4070–4075.
12. **Korchak, H. M., K. Vienne, L. E. Rutherford, C. Wilkenfeld, M. C. Finkelstein, and G. Weissmann.** 1984. Stimulus response coupling in the human neutrophil. II. Temporal analysis of changes in cytosolic calcium and calcium efflux. J. Biol. Chem. **259**:4076–4082.
13. **Kruskal, B. A., S. Shak, and F. R. Maxfield.** 1986. Spreading of human neutrophil is immediately preceded by a large increase in cytoplasmic free calcium. Proc. Natl. Acad. Sci. USA **83**:2919–2923.
14. **Lew, P. D., A. Monod, F. A. Waldvogel, B. Dewald, M. Baggiolini, and T. Pozzan.** 1986. Quantitative analysis of cytosolic free calcium dependency of exocytosis from three subcellular compartments in intact human neutrophils. J. Cell Biol. **102**:2197–2204.
15. **Lew, P. D., C. B. Wollheim, F. A. Waldvogel, and T. Pozzan.** 1984. Modulation of cytosolic free calcium transients by changes in intracellular calcium-buffering capacity: correlation with exocytosis and O_2^- production in human neutrophils. J. Cell Biol. **99**:1212–1220.
16. **Mandell, G. L.** 1971. Influence of type of ingested particle on human leukocyte metabolism. Proc. Soc. Exp. Biol. Med. **137**: 1228–1230.
17. **Maridonneau-Parini, I., S. M. Tringale, and A. I. Tauber.** 1986. Identification of distinct activation pathways of the human neutrophil NADPH-oxidase. J. Immunol. **137**:2925–2929.
18. **McNeil, P. L., J. A. Swanson, S. D. Wright, S. C. Silverstein, and D. L. Taylor.** 1986. Fc-receptor-mediated phagocytosis occurs in macrophages without an increase in average $[Ca^{2+}]_i$. J. Exp. Med. **102**:1586–1592.
19. **Melloni, E., S. Pontremoli, M. Michetti, O. Sacco, B. Sparatore, F. Salamino, and B. L. Horecker.** 1985. Binding of protein kinase C to neutrophil membranes in the presence of Ca^{2+} and its activation by a Ca^{2+}-requiring proteinase. Proc. Natl. Acad. Sci. USA **82**:6435–6439.
20. **Myers, M. A., L. C. Mcphail, and R. Snyderman.** 1985. Redistribution of protein kinase C activity in human monocytes: correlation with activation of the respiratory burst. J. Immunol. **135**:3411–3416.
21. **Naccache, P. H., M. Volpi, H. J. Showell, E. L. Becker, and R. I. Sha'afi.** 1979. Chemotactic factor-induced release of membrane calcium in rabbit neutrophils. Science **203**:461–463.
22. **Romeo, D., G. Zabucchi, N. Miani, and F. Rossi.** 1975. Ion movement across leukocyte plasma membrane and excitation of their metabolism. Nature (London) **253**:542–544.
23. **Roos, D., A. A. M. Bot, M. L. J. van Schaik, M. deBoer, and M. R. Daha.** 1981. Interaction between human neutrophils and zymosan particles: the role of opsonins and divalent cations. J. Immunol. **126**:433–440.
24. **Ross, G. D., J. A. Cain, and P. J. Lachmann.** 1985. Membrane complement receptor type three (CR_3) has lectin-like properties analogous to bovine conglutinin and functions as a receptor for zymosan and rabbit erythrocytes as well as a receptor for iC3b. J. Immunol. **134**:3307–3315.
25. **Salata, R. A., J. A. Sullivan, and G. L. Mandell.** 1983. Visualization of hydrogen peroxide in living polymorphonuclear neutrophils utilizing leucodiacetyl 2',7'-dichlorofluorescin: photomicrographic and microphotometric studies. Trans. Assoc. Am. Physicians **96**:375–383.
26. **Sawyer, D. W., J. A. Sullivan, and G. L. Mandell.** 1985. Intracellular free calcium localization in neutrophils during phagocytosis. Science **230**:663–666.
27. **Smolen, J. E., H. M. Korchak, and G. Weissmann.** 1981. The roles of extracellular and intracellular calcium in lysosomal enzyme release and superoxide anion generation by human neutrophils. Biochim. Biophys. Acta **677**:512–520.
28. **Stossel, T. P.** 1973. Quantitative studies of phagocytosis: kinetic effects of cations and heat-labile opsonin. J. Cell Biol. **58**:346–356.
29. **Stossel, T. P., R. J. Field, J. D. Gitlin, C. A. Alper, and F. S. Rosen.** 1975. The opsonic fragment of the third component of human complement (C3). J. Exp. Med. **141**:1329–1347.
30. **Suzuki, H., M. J. Pabst, and R. B. Johnston, Jr.** 1985. Enhancement by Ca^{2+} or Mg^{2+} of catalytic activity of the superoxide-producing NADPH oxidase in membrane fractions of human neutrophils and monocytes. J. Biol. Chem. **260**:3635–3639.
31. **Tsien, R. Y., T. J. Rink, and M. Poenie.** 1985. Measurement of cytosolic free Ca^{2+} in individual small cells using fluorescence microscopy with dual excitation wavelengths. Cell Calcium **6**:145–157.
32. **Young, J. D. E., J. C. Unkeless, T. M. Young, A. Mauro, and Z. A. Cohn.** 1983. Role for mouse macrophage IgG Fc receptor as ligand-dependent ion channel. Nature (London) **306**:186–189.